

Stationary-state skewness in two-dimensional Kardar-Parisi-Zhang type growth

Chen-Shan Chin and Marcel den Nijs

Department of Physics, University of Washington, P.O. Box 351560, Seattle, Washington 98195-1560

(Received 6 October 1998)

We present numerical Monte Carlo results for the stationary-state properties of KPZ-type growth in two-dimensional surfaces, by evaluating the finite size scaling (FSS) behavior of the second and fourth moments W_2 and W_4 and the skewness W_3 in the Kim-Kosterlitz (KK) and body-centered solid-on-solid (BCSOS) models. Our results agree with the stationary state proposed by Lässig. The roughness exponents $W_n \sim L^{\alpha_n}$ obey power counting $\alpha_n = n\alpha$, and the amplitude ratios of the moments are universal. They have the same values in both models: $W_3/W_2^{1.5} = -0.27(1)$ and $W_4/W_2^2 = +3.15(2)$. Unlike in one dimension, the stationary-state skewness is not tunable, but a universal property of the stationary-state distribution. The FSS corrections to scaling in the KK model are weak and α converges well to the Kim-Kosterlitz-Lässig value $\alpha = \frac{2}{5}$. The FSS corrections to scaling in the BCSOS model are strong. Naive extrapolations yield a smaller value $\alpha \approx 0.38(1)$, but are still consistent with $\alpha = \frac{2}{5}$ if the leading irrelevant corrections to the FSS scaling exponent are of order $y_{ir} \approx -0.6(2)$. [S1063-651X(99)00503-6]

PACS number(s): 02.50.Ey, 05.40.-a, 68.35.Fx

I. INTRODUCTION

KPZ-type growth is one of the generic dynamic processes describing the growth of crystal surfaces. It is named after the Langevin equation introduced by Kardar, Parisi, and Zhang about a decade ago [1–5]:

$$\frac{\partial h}{\partial t} = \nu \frac{\partial h^2}{\partial x^2} + \lambda \left(\frac{\partial h}{\partial x} \right)^2 + \eta, \quad (1)$$

with h the surface height and η uncorrelated noise

$$\langle \eta(x_1, t_1) \eta(x_2, t_2) \rangle = D \delta(t_1 - t_2) \delta(x_1 - x_2). \quad (2)$$

Numerous microscopic models on the master equation level have been studied numerically as well and are confirmed to be in the KPZ universality class [2–5]. However, many properties of this process are still in question, including basic aspects, like the precise values of the scaling critical exponents and the detailed structure of the stationary growing state. Part of the problem is the absence of an obvious mean field theory. The linear, integrable diffusion, part of the KPZ equation ($\lambda = 0$) does not play the role of mean field theory fixed point in high enough dimensions (D). The KPZ behavior is governed by a strong coupling fixed point for all D , and thus evades perturbative renormalization treatments [6].

It is widely accepted that the dynamic exponent z and the stationary-state roughness exponent α obey the equality $\alpha + z = 2$ in all D [2–5]. These critical exponents specify how time and height rescale under a renormalization transformation $x \rightarrow bx$, $t \rightarrow b^z t$, and $h \rightarrow b^\alpha h$. The exponent identity states that under renormalization the amplitude of the non-linear term in the KPZ equation does not change. λ is a so-called redundant scaling field. It plays a role similar to lattice anisotropy in equilibrium phase transitions. Increasing λ simply speeds up the process, and scaling amplitudes are

proportional to λ . This exponent equality links the dynamic scaling to the stationary state scaling. Therefore the focus has shifted recently to the structure of the stationary state.

The stationary growing state is trivial in one dimension (1D). It is the Gaussian distribution. The up and down steps along the surface are uncorrelated beyond a definite correlation length. This implies $\alpha = \frac{1}{2}$ (the random walk value), and from the above exponent identity it follows that $z = \frac{3}{2}$. This behavior is well established, not only by numerical studies [2–5], but also analytically. The 1D body-centered solid-on-solid (BCSOS) growth model is exactly soluble [7,8]. Its master equation is a special case of the 2D equilibrium six-vertex model. In the latter representation, KPZ scaling describes facet ridge end points of equilibrium crystal shapes [9]. One-dimensional KPZ growth is equivalent also to asymmetric exclusion hopping processes [10]. Moreover, the exact stationary state of the Langevin equation itself is known in 1D and is indeed the Gaussian distribution [5].

The stationary state is not simple in $D > 1$. The stationary-state roughness exponent α takes a nontrivial value and is actually not very well known numerically. For example, in 2D the reported values vary between $\alpha = 0.37$ and 0.4 [3,4,11–13]. Lässig made an important analytical breakthrough last year [14]. He proposed the likely structure of the stationary state by studying the operator product expansion of the (height variable) correlation functions. Under the assumption that the algebra closes and contains only one scaling field operator, Lässig obtained a quantization condition for the exponents. One of these solutions, $\alpha = \frac{2}{5}$, is close to the above 2D numerical values. The moments

$$W_n = \langle (h_i - \bar{h})^n \rangle \quad (3)$$

of Lässig's stationary-state distribution obey power counting; i.e., the exponents in the scaling relations

$$W_n(N^{-1}, t^{-1}) = b^{\alpha n} W_n(bN^{-1}, b^z t^{-1}) \quad (4)$$

are related as $\alpha_n = n\alpha$. The distribution lacks multiscaling. Moreover, for the closure of the algebra it is important that the stationary state be skewed. The odd moments, in particular the third one, must be nonzero.

In this paper we report a detailed numerical study of the stationary state in 2D for the Kim-Kosterlitz (KK) [11] and the BCSOS model. We determine the finite-size scaling behavior of the second, third, and fourth moments.

In Sec. II we review the properties of stationary-state skewness in 1D KPZ growth, and list the possibilities in higher dimensions. Section III contains our numerical results for the KK and BCSOS models. The third moment is indeed nonzero and the second, third, and fourth moments indeed obey power counting. We find strong evidence that the amplitude ratios of the moments are universal, $R_3 = W_3/W_2^{1.5} = -0.27(1)$ and $R_4 = W_4/W_2^2 = +3.15(2)$. The amount of stationary-state skewness is the same in these two models. In 1D skewness is tunable, but appears not to be so in 2D. The values of these amplitude ratios are the major new results of this paper.

One of the major differences between this and most earlier numerical studies of KPZ-type growth is our detailed corrections to the finite-size scaling (FSS) analysis. This allows us to address in Sec. III whether the differences between the previous reported values of α for the KK and BCSOS models can be attributed to FSS-type corrections. The leading FSS scaling corrections to the scaling exponent are large for the even moments and in the range of values predicted by naive power counting.

To check more directly whether skewness is tunable or not, we introduce a temperature-type parameter K in the BCSOS model. In the KK model it is known that λ changes sign with K [12]. In Sec. IV we give an intuitive explanation for why this happens. (It is related to preroughening phenomena in equilibrium surfaces.) In the BCSOS model λ does not change sign. In Sec. V we present Monte Carlo (MC) data for the K dependence of the roughness exponents and the amplitude ratios. Both show some systematic drift, but much smaller than expected if they would vary with K .

II. STATIONARY-STATE SKEWNESS

This study was actually not motivated by Lässig's recent results. It was conceived as a generalization of an earlier study of stationary-state skewness in 1D [15]. The KK model is a special point in the restricted solid-on-solid (RSOS) model. We varied its adsorption and evaporation probabilities in the 1D model by making them dependent on the local nearest-neighbor heights. That led to five independent parameters. Surprisingly we were able to construct the exact stationary state in a four-dimensional subspace. Its structure is simple. The steps in the interface are completely uncorrelated. Only the step density varies. This state has zero skewness. It is a Gaussian and has particle-hole symmetry. Outside this exact soluble subspace the stationary state is skewed. This means that in general KPZ-type growth in 1D has a nonzero third moment W_3 in its stationary state. For example, the KK point lies outside the nonskewed subspace. On the other hand, the stationary states in the exactly soluble BCSOS model and also the Langevin equation itself are nonskewed. Stationary-state skewness is distinct from temporal

skewness. Most initial states develop into skewed structures at intermediate time scales (temporal skewness) even if the stationary state is not skewed [16].

So in 1D, KPZ-type stationary states are typically skewed, and its amplitude is tunable. This raises the immediate question of whether skewness affects the scaling exponents. Let us refer to the operators leading out of the nonskewed subspace as \mathcal{O}_{sk} and to their conjugate coupling constants as u_{sk} . In 1D, a KPZ-type fixed point with zero skewness exists. The question is whether this fixed point is stable and whether \mathcal{O}_{sk} is a relevant, marginal, redundant, or an irrelevant operator. Suppose the nonskewed KPZ fixed point is stable. The moments should scale then with system size as

$$W_n(N^{-1}, u_{\text{sk}}) = b^{\alpha_n} W_n(bN^{-1}, b^{y_{\text{sk}}} u_{\text{sk}}), \quad (5)$$

with $\alpha_n = n\alpha$ and $y_{\text{sk}} < 0$. All even moments scale as

$$W_n \simeq AN^{\alpha_n} + \dots, \quad (6)$$

with universal amplitude ratios $R_n = W_n/W_2^{n/2}$. All odd moments scale as

$$\begin{aligned} W_n(N^{-1}, u_{\text{sk}}) &= N^{\alpha_n} \mathcal{F}_n(N^{y_{\text{sk}}} u_{\text{sk}}) \\ &= N^{\alpha_n} [\mathcal{F}_n(0) + \mathcal{F}'_n(0) N^{y_{\text{sk}}} u_{\text{sk}} + \dots] \\ &\sim u_{\text{sk}} N^{\alpha_n + y_{\text{sk}}}, \end{aligned} \quad (7)$$

with $\mathcal{F}_n(0) = 0$ because the fixed point has no skewness. The odd amplitude ratios are proportional to u_{sk} ; i.e., the skewness varies continuously.

Numerical (transfer matrix finite size scaling) results confirmed that the nonskewed KPZ fixed point is stable in 1D. We found $y_{\text{sk}} \simeq -1$. Moreover, the amplitude of W_3 (at, e.g., the KK point) is indeed roughly proportional to the skewness coupling constant u_{sk} , in accordance with Eq. (7).

We performed a mean-field-type analysis of the master equations [15]. This identifies the crossover operator \mathcal{O}_{sk} with interactions like $(\partial^2 h / \partial x^2)^2$ that break particle-hole symmetry. The latter interaction has as naive scaling dimension $y_{\text{ir}} = -2$ (by power counting with $\alpha = \frac{1}{2}$ and $z = 2 - \alpha = \frac{3}{2}$). This is smaller than the observed value. We failed to find an operator in the KPZ equation with power-counting scaling dimension $y_{\text{ir}} = -1$. The origin of the corrections to scaling with $y_{\text{ir}} = -1$ remains therefore somewhat of a puzzle. However, there is room for additional irrelevant operators not represented in the Langevin equation. For example, the combination of the discreteness of the height variables, the lattice, and the RSOS restriction gives rise to an additional order parameter, the step density, besides the local slope in the mean field analysis [15]. We found that the step density is a massive field with a definite short relaxation time scale, and therefore can be integrated out. However, it can be the origin of additional irrelevant operators.

Skewness is negative at the 1D KK point. On average hill tops are wider (flatter, less sharp) than valley bottoms. Such a statement is meaningless without the specification of a cut-off. The definition of what constitutes a mountain and what represents a local hump depends on the length scale at which

the surface configuration is being viewed. (Humans do not interpret every grain of sand as a hill.) Skewness is a scale-dependent property. The asymptotic scaling of the moments tells us how asymmetric the hills and valleys are in the large length scale limit. In 1D this skewness persists all the way to microscopic length scales. We calculated the surplus of sharp valley bottoms over sharp hill tops at the microscopic (the grains of sand) level. This expectation value has the same sign as the macroscopic skewness and is also roughly proportional to u_{sk} . This invariance of the surface structure over all length scales is related to the rather trivial nature of the fixed-point stationary state (Gaussian distribution).

The tunability of the skewness at the microscopic length scale is easy to understand. Consider the 1D RSOS model with deposition only, with three parameters p_h , p_s , and p_v [15]. The density of local sharp hill tops is set by the deposition probability p_h of particles on local flat surface segments. The sharpness of these local hill tops is set by the rate at which they broaden, i.e., the probability with which particles adhere to existing steps, p_s . The density of local sharp valleys is set by the rate at which single-particle puddles fill up, p_v , compared to the rate at which they are created, $2p_s$. These processes balance exactly inside the subspace where the stationary state is trivial and has zero skewness. At the KK point $p_h = p_s = p_v = 1$, the balance is imperfect and the dynamics creates a backlog of “to-be-filled-up” local valleys. Newly created local hill tops broaden readily, and therefore are flatter [15].

Is the skewness tunable in $D > 1$ as well? Is there maybe a line of KPZ-type fixed points with continuously varying skewness? A varying exponent α would explain the current numerical spread in its value. Is it possible to change the sign of skewness without changing the sign of λ in Eq. (1)? Or is there one single KPZ stationary-state fixed-point distribution, with a universal amount (and sign) of skewness? In that case we need to explain the numerical spread in α 's in terms of strong FSS corrections. These are the issues we address in this paper.

III. SCALING OF THE STATIONARY-STATE MOMENTS

We perform a systematic numerical study of the stationary-state properties in the 2D KK model and the BC-SOS model. In both cases we allow only particle deposition (no desorption). Consider a 2D square lattice with a height variable $h(r) = 0, \pm 1, \pm 2, \dots$ at each lattice site. We apply periodic boundary conditions. In the KK model, nearest-neighbor columns are allowed to differ by at most one unit, $\delta h = 0, \pm 1$. Choose a site at random, and deposit a particle $h \rightarrow h + 1$, with probability $p = 1$, unless such a move would violate the above restriction.

In the BCSOS model the square lattice is divided into two sublattices. The height variables are restricted to be even on one of them, $h(r) = 0, \pm 2, \dots$, and to be odd on the other, $h(r) = \pm 1, \pm 3, \dots$, such that nearest-neighbor columns always differ in height by one $\delta h = \pm 1$. Choose at random a site, and deposit a particle with probability $p = 1$ if the move does not violate the $\delta h = \pm 1$ constraint. In Sec. V we consider also the generalization where the BCSOS deposition probabilities vary with the local configuration by means of a temperature type parameter, $p = \min(1, \exp(-\Delta E))$. Here ΔE

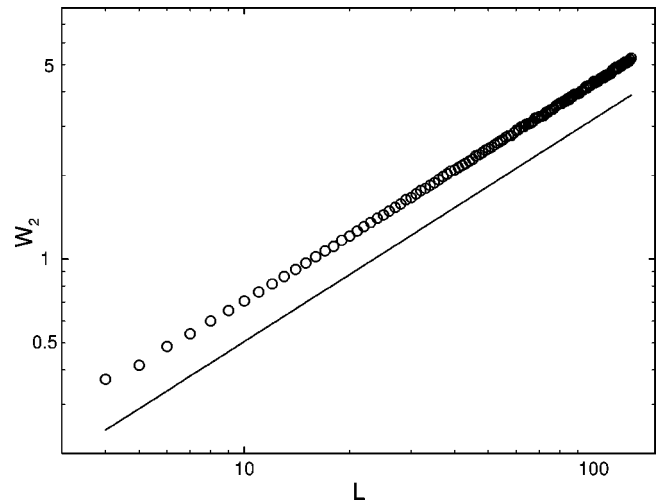


FIG. 1. Stationary-state second moment W_2 of the 2D Kim-Kosterlitz (KK) model as function of lattice size L^2 . The solid line with slope 0.8 is shown as reference.

is the energy change if the adsorption would take place. The energy

$$E(\{h_i\}) = \sum_{\langle i,j \rangle} \frac{1}{4} K (h_i - h_j)^2 \quad (8)$$

has a tunable parameter K and the summation runs over all next nearest neighbors. This rule is identical to that in standard Metropolis MC simulations, except that desorption is forbidden. The latter breaks detailed balance and leads to the nonequilibrium growing stationary state.

We determine the second, third, and fourth moments of the stationary states. The MC averages in this section involve $\approx 2 \times 10^6$ MC steps, after $\approx 4 \times 10^3$ initial MC configurations, to allow the surface to reach its stationary state. The square lattice size L^2 varies as $12 \leq L \leq 128$.

First consider the KK model. Figure 1 shows the second moment W_2 . It scales as $W_2 \approx AL^{\alpha_2}$. The slope of the log-log plot gives the exponent α_2 . It is a mistake to apply a least-squares-type fit to the slope at large L . One should determine the slope at various system size intervals and perform a FSS analysis. Figure 2 represents such an analysis. It shows FSS estimates for α_2 from the same data, defined as $\alpha_2(L) = \ln[W_2(L_2)/W_2(L_1)] / \ln[L_2/L_1]$ with $L_2 \approx 1.2L_1$ and $L = \frac{1}{2}(L_1 + L_2)$. Such a FSS scaling analysis is only barely feasible at large system sizes due to the intrinsic MC noise. Figure 2 is indeed rather noisy at large L . The MC scatter increases with system size, since the stationary state is intrinsically critical and therefore subject to a critical slowing down. We opted for running many lattice sizes instead of fewer but longer MC runs. The solid line is obtained by averaging the $\alpha_2(L)$ locally, over $L - 7 \leq L \leq L + 7$. The data in Fig. 2 converge by eye to $\alpha_2 = 0.80(2)$, consistent with the value $\alpha = \frac{2}{5}$ proposed by Kim and Kosterlitz from their earlier numerical results [11,12] and with Lässig's [14] stationary state. The FSS corrections to scaling in the KK model are small compared to the MC noise.

Figures 3 and 4 show the same FSS analysis for the third and fourth moment exponents α_3 and α_4 . They converge by eye to $\alpha_3 = 1.20(4)$ and $\alpha_4 = 1.60(5)$. The corrections to

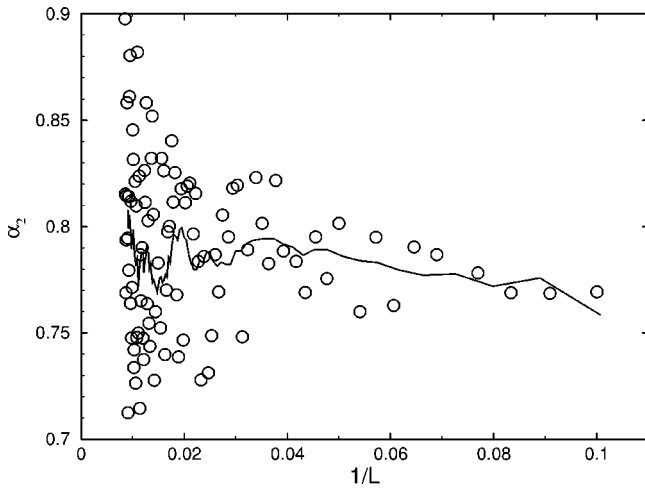


FIG. 2. Finite-size scaling approximants for the surface roughness exponent α_2 of the second moment, $W_2 \approx AL^{\alpha_2}$, in the stationary state of the 2D KK model.

FSS are again small compared to the MC noise. The surface is skewed and power counting, $\alpha_n = n\alpha$, is satisfied within the numerical accuracy.

Figures 5 and 6 show the amplitude ratios (the circles) of the third and fourth moments compared to the second one, $R_n = W_n / (W_2)^{n/2}$. The fact that these ratios convergence gives additional evidence of the validity of power-counting. Actually, they do so much smoother than the exponents α_n , suggesting that the MC fluctuations tend to preserve the power counting property better than the precise value of α . The amplitude ratios converge smoothly to $R_3 = -0.27(1)$ and $R_4 = +3.15(2)$. Skewness is negative, $R_3 < 0$. It is probably wishful thinking to guess that $R_4 = \pi$. ($R_4 = 3$ in Gaussian distributions.)

The above results demonstrate that in 2D the amplitudes $\mathcal{F}_n(0)$ in Eq. (7) do not vanish for the odd moments. In 1D, the KPZ fixed point lies at zero skewness; in 2D it has non-zero skewness. This agrees with Lässig's [14] stationary state. However, the amplitude ratios must be universal if the

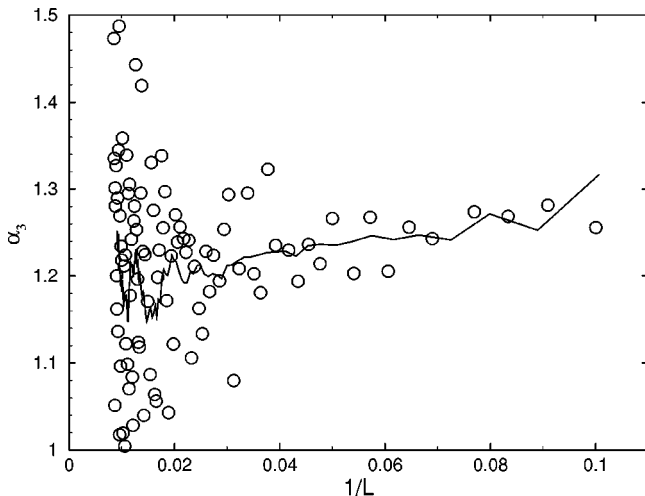


FIG. 3. Finite-size scaling approximants $\alpha_3(L)$ for the surface roughness exponent α_3 of the third moment, $W_3 \approx AL^{\alpha_3}$, in the stationary state of the 2D KK model.

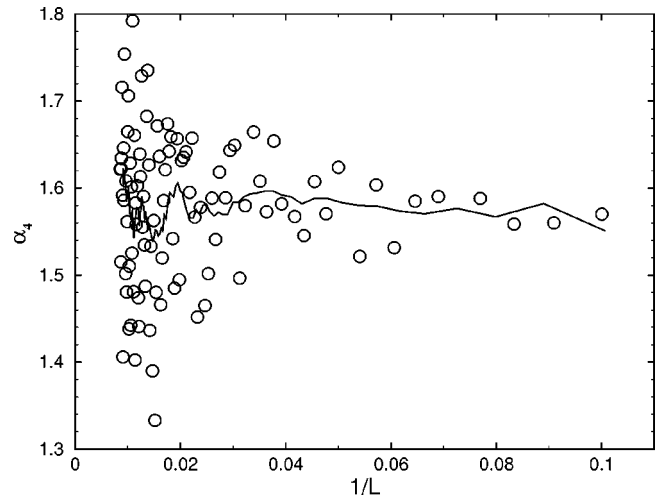


FIG. 4. Finite-size scaling approximants $\alpha_4(L)$ for the surface roughness exponent α_4 of the fourth moment, $W_4 \approx AL^{\alpha_4}$, in the stationary state of the 2D KK model.

KPZ scaling behavior is described by one single fixed point. To check this we repeat the same analysis for the BCSOS model.

Consider the BCSOS model at $K=0$. Figures 7, 8, and 9 show the same type of FSS estimates for the exponents α_n . The finite-size corrections to scaling are much larger than in the KK model. The data converge by eye systematically to smaller values than in the KK model: $\alpha_2 = 0.77(2)$, $\alpha_3 = 1.16(3)$, and $\alpha_4 = 1.54(4)$. This is consistent with the value for α_2 reported in the literature [4,13]. These α_n 's are mutually consistent with power counting. Power counting is again more stable than the values of the exponents α_n . Most importantly, the amplitude ratios in Figs. 5 and 6 (diamonds) converge to the same values as in the KK model (circles).

Is α really smaller than in the KK model and different from the Kim-Kosterlitz-Lässig (KKL) value? The finite-size scaling corrections in the BCSOS model are several orders of magnitude bigger than in the KK model. Is it believable that these apparent differences are due to corrections to scaling

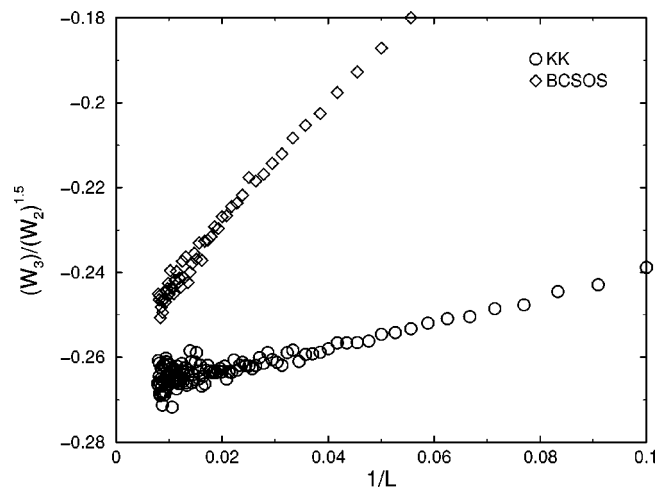


FIG. 5. Finite-size scaling behavior of the skewness amplitude ratio $R_3 = W_3 / W_2^{1.5}$ in the 2D KK model (circles) and the $K=0$ BCSOS model (diamonds).

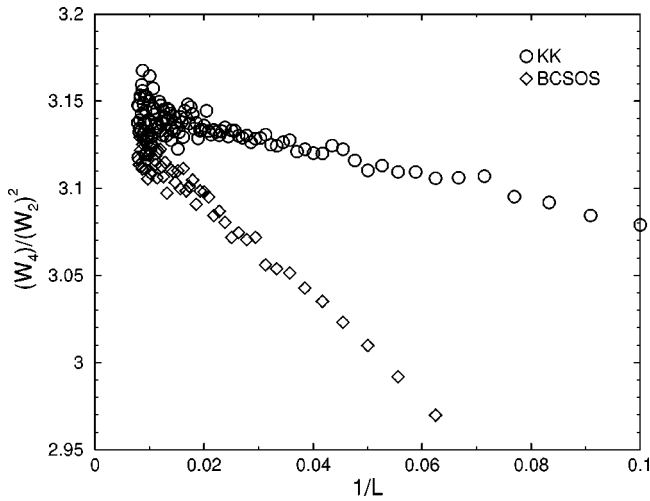


FIG. 6. Finite-size scaling behavior of the fourth-moment amplitude ratio $R_4 = W_4/W_2^2$ in the 2D KK model (circles) and the $K=0$ BCSOS model (diamonds).

only? The above FSS extrapolation “by eye” presumes implicitly that all α_n converge approximately linearly in L^{-1} . This looks reasonable from the data, but is too restrictive. Corrections to scaling originate from so-called irrelevant scaling fields. The corrections to scaling exponents $y_{\text{ir}} < 0$ in $W_n \approx A_n N^{\alpha_n} [1 + B_n L^{y_{\text{ir}}} + \dots]$ are universal properties of the stationary-state fixed point. The amplitudes B_n are not universal. They depend on the “distance” of the model to the fixed point and the quantity we are looking at. Assume that one correction to scaling term dominates, i.e., that all other operators scale with much more negative values of y_{ir} . The same exponent y_{ir} should then appear in all moments. The only exception is that in specific quantities the leading term might have zero amplitude by symmetry. For example, all even moments might show a different leading exponent y_{ir} than all odd ones. This actually happens here.

Suppose we force our BCSOS data to converge to $\alpha = \frac{2}{5}$. We made plots of $W_n/L^{n\alpha}$ with $\alpha = \frac{2}{5}$ versus $L^{y_{\text{ir}}}$ for a range of values of y_{ir} . This should be a straight line at the proper y_{ir} . From this we estimate that $y_{\text{ir}} \approx -0.6(2)$ for the

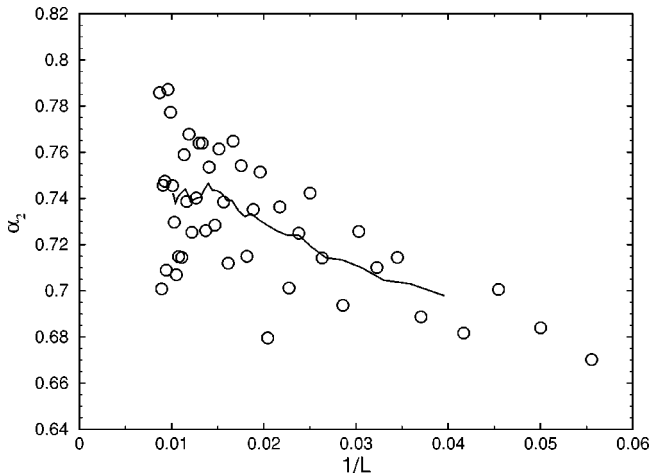


FIG. 7. Finite-size scaling approximants for the surface roughness exponent α_2 of the second moment, $W_2 \approx AL^{\alpha_2}$, in the stationary state of the 2D BCSOS model.

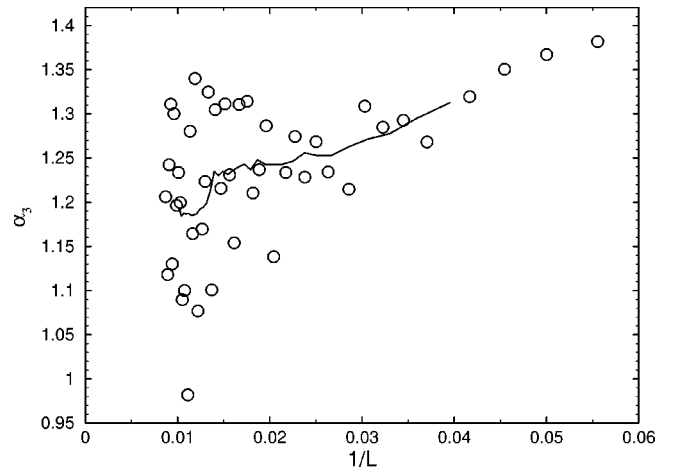


FIG. 8. Finite-size scaling approximants for the surface roughness exponent α_3 of the third moment, $W_3 \approx AL^{\alpha_3}$, in the stationary state of the 2D BCSOS model.

second and fourth moments, and $y_{\text{ir}} \approx -1.7(3)$ for the third moment. These straight line fits are satisfactory stable. So the KKL value for α is within the realm of possibilities for the BCSOS model. Still, it remains a leap of faith, because the curves in Figs. 7, 8, and 9 are bent to the limit.

It would be much more convincing if the corrections to scaling exponents were known analytically and/or take simple values. At the core of Lässig’s result is the assumption that the operator content of the system is simple. Therefore one would expect that the irrelevant operators have rather trivial critical dimensions, like integers, multiples of α , and combinations of both. The above numerical values of y_{ir} do not look that simple, but are of the same order of magnitude as we might expect. Simpleminded power counting in Eq. (1), with $\alpha = \frac{2}{5}$ and $z + \alpha = 2$, suggests that the corrections to scaling are strong and that the curvature operator $\partial^2 h / \partial x^2$ is irrelevant, but not by much, $y_{\nu} = -\alpha$. The corrections to FSS in the third moment are much smaller. The curvature operator $\partial^2 h / \partial x^2$ does not affect it and probably all other operators that change sign under $h \rightarrow -h$ either. One of the leading remaining candidates is $(\partial^2 h / \partial x^2)^2$

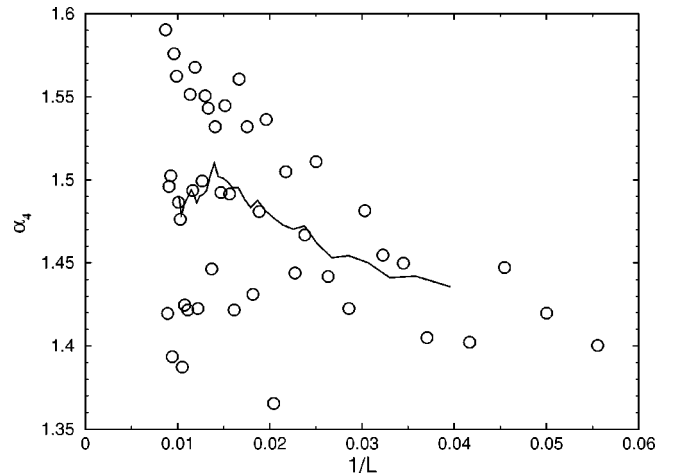


FIG. 9. Finite-size scaling approximants for the surface roughness exponent α_4 of the fourth moment, $W_4 \approx AL^{\alpha_4}$, in the stationary state of the 2D BCSOS model.

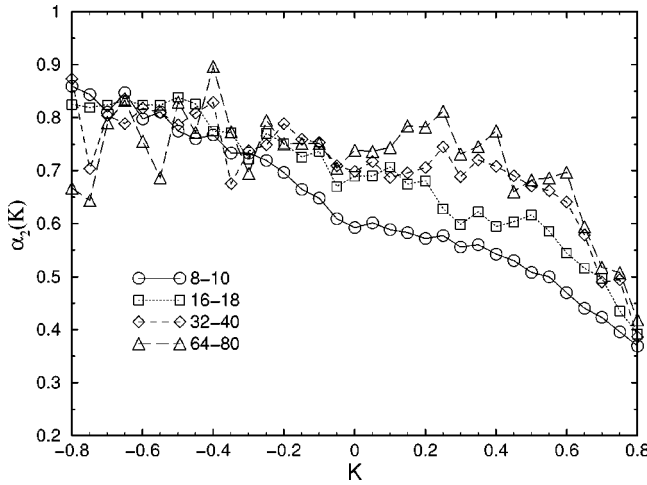


FIG. 10. Finite-size scaling approximants for the surface roughness exponent α_2 of the second moment, $W_2 \approx AL^{\alpha_2}$, in the stationary state of the 2D BCSOS model as function of K .

which we associated with skewness in the 1D model (see Sec. II). It gives rise to $y_{sk} = -2$.

IV. TEMPERATURE-DEPENDENT TRANSITION PROBABILITIES

In Sec. V we vary the temperature-type parameter K in the BCSOS model, to study the universality of α and skewness issues raised in Sec. III in more detail. We do this only for the BCSOS model, not the RSOS model. (The KK model is a special point in the phase diagram of latter.) From earlier studies it is known that in the RSOS model the KPZ nonlinear term λ changes sign with K [12]. This creates strong Edwards-Wilkinson- (EW-) type corrections to scaling and will obscure the skewness property, because the EW stationary state at $\lambda = 0$ is nonskewed (the Gaussian distribution). Such a change in λ does not take place in the BCSOS model.

The following connection with preroughening phenomena in equilibrium crystal surface explains why λ changes sign in the RSOS model and not in the BCSOS model. Imagine a two-dimensional phase diagram, with $K \sim T^{-1}$ the temperaturelike parameter and a parameter s representing the asymmetry between particle deposition and evaporation. $s = 0$ corresponds to MC-equilibrium-type dynamics and $s = 1$ to the above pure deposition model without evaporation. The equilibrium surface undergoes a roughening transition. The rough phase is the EW stationary state. The scaling properties of the equilibrium (stationary) state are described by the Gibbs distribution of the sine-Gordon model:

$$E = \int dx dy \left[\frac{K}{2} (\nabla h)^2 + u_2 \cos(2\pi h) + u_4 \cos(4\pi h) \right]. \quad (9)$$

It is known that u_2 varies with temperature and changes sign inside the equilibrium rough phase in the RSOS model just above the roughening transition. This follows from an exact duality transformation [17]. The location of this $u_2 = 0$ point at $s = 0$ agrees qualitatively with the numerical value of the $\lambda = 0$ point at $s = 1$. Those values do not have to be identical.

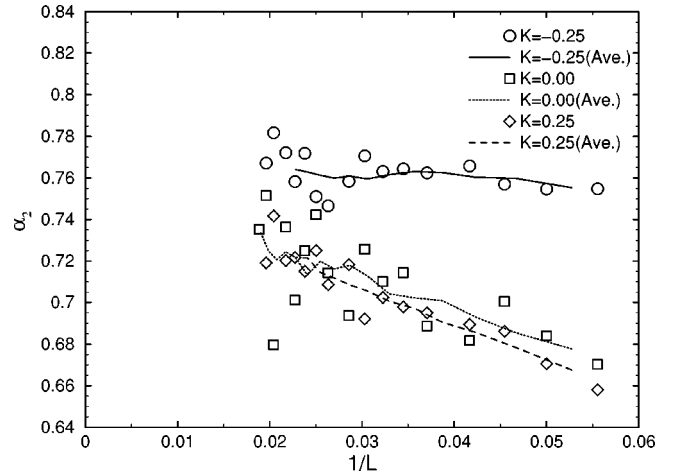


FIG. 11. Finite-size scaling approximants for the surface roughness exponent α_2 of the second moment in the stationary state of the 2D BCSOS model at $K = \pm 0.25$ and 0.

They only need to be of the same order of magnitude. The following arguments suggest that a line of $\lambda = 0$ points emerges from the $u_2 = 0$ point at $s = 0$ into the s direction.

u_2 is negative at the high-temperature side of the $u_2 = 0$ line. There, the rough stationary-state surface takes locally the so-called disordered-flat-type structure with alternating up and down steps and local half-integer surface height [18]. This is the same surface structure as in the BCSOS model (but not close packed with $dh = \pm 1$ kinks). The nonlinear term in the KPZ equation controls the local growth velocity at sloped sections of the surface. Growth at slopes is suppressed in BCSOS-type rough structures, and therefore $\lambda < 0$. At the opposite, low-temperature $u_2 > 0$ side of the $u_2 = 0$ point, the local rough RSOS surface is smooth, and has on the local level integer average surface heights. In such structures, growth at sloped parts of the surface is enhanced and therefore $\lambda > 0$.

The location of $u_2 = 0$ can be controlled by introducing further neighbor interactions. This point transforms into the preroughening transition point when it moves below the

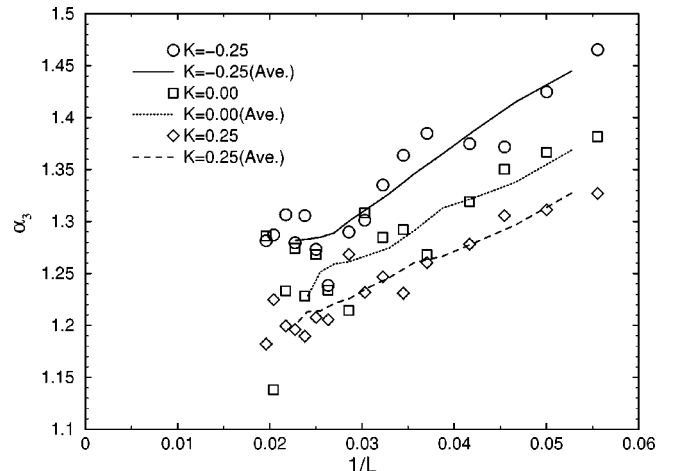


FIG. 12. Finite-size scaling approximants for the surface roughness exponent α_3 of the third moment in the stationary state of the 2D BCSOS model at $K = \pm 0.25$ and 0.

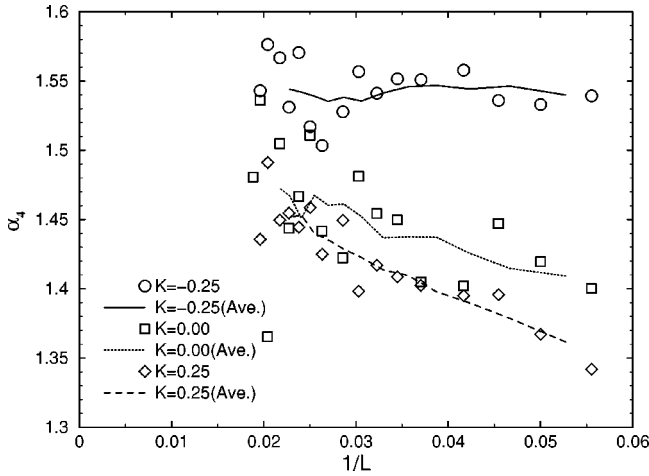


FIG. 13. Finite-size scaling approximations for the surface roughness exponent α_4 of the fourth moment in the stationary state of the 2D BCSOS model at $K = \pm 0.25$ and 0.

roughening temperature [18] (but only at $s \neq 0$, because the driven nonequilibrium surface is always rough).

Such a change in λ does not take place in the BCSOS model. Its equilibrium stationary state (at $s = 0$) is exactly known for all K from the exact solution of the six-vertex model [19]. u_2 is negative at all values of K in the $s = 0$ equilibrium surface. Therefore there is no reason to expect a change of λ as a function of K in the pure deposition model at $s = 1$. This makes the BCSOS model a suitable testing ground for the tunability of 2D skewness and the universality of α .

V. TEMPERATURE-DEPENDENT DEPOSITION RATES IN THE BCSOS MODEL

In this section we study the universality of the stationary-state roughness exponent α and the skewness by varying the deposition probabilities in the BCSOS model. This should clarify whether the skewness is truly universal or a tunable

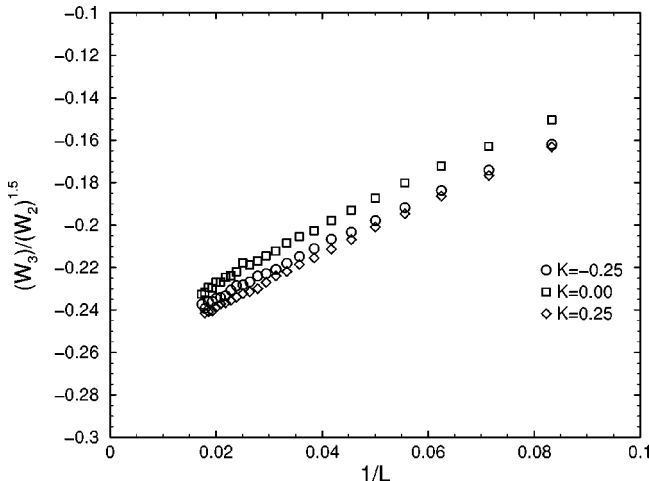


FIG. 14. Finite-size scaling behavior of the skewness amplitude ratio $R_3 = W_3/W_2^{1.5}$ in the stationary state of the 2D BCSOS model at $K = \pm 0.25$, and 0.

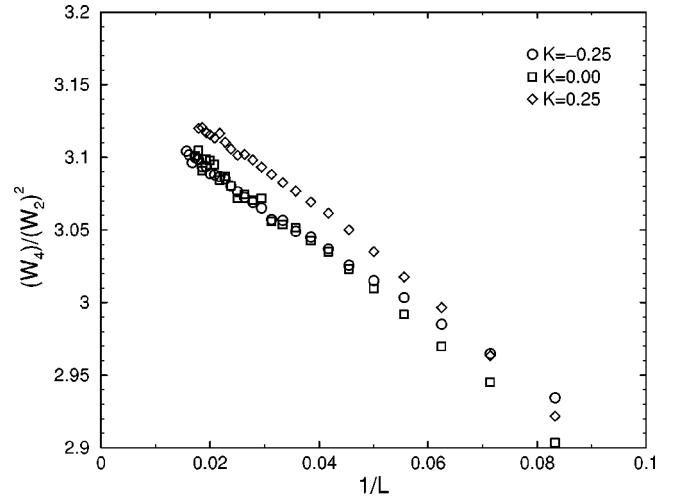


FIG. 15. Finite-size scaling behavior of the fourth moment amplitude ratio W_4/W_2^2 in the stationary state of the 2D BCSOS model at $K = \pm 0.25$ and 0.

parameter. We can control the microscopic particle-hole asymmetry explicitly.

Figure 10 shows the variation of the second-moment exponent $\alpha_2(L)$ with the temperature parameter K . This plot is more qualitative than the ones in Sec. III. The system sizes are smaller (up to $L = 80$) and the MC runs an order of magnitude shorter (up to 10^5 MC steps, after 2500 initial MC steps). The curves have a definite slope at small system sizes, but these disappear with system size. At temperatures beyond $K \approx 1$ the surface becomes very flat and inactive. Compared to $K \approx 0$ the system size is effectively much smaller and the MC runs effectively much shorter. This explains the decay in the approximants at large K . At the opposite side, beyond $K \approx -1$, the surface becomes quite faceted at short distances and the dynamics slows down again. Faceted structures have $\alpha = 1$. This explains why the $\alpha_2(L)$ curves drift upward on the left hand side in Fig. 10. Here α_3 and α_4 vary also only weakly with K . The amplitude ratios R_3

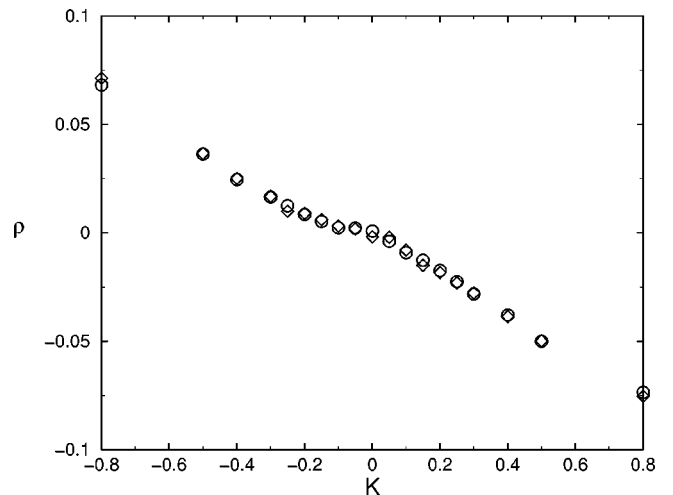


FIG. 16. The difference in the expectation value of local sharp hill tops and of local sharp valley bottoms as function of K in the 2D BCSOS model along 1D cross sections through the surface. The diamonds (circles) are for lattice size $L = 36$ (64).

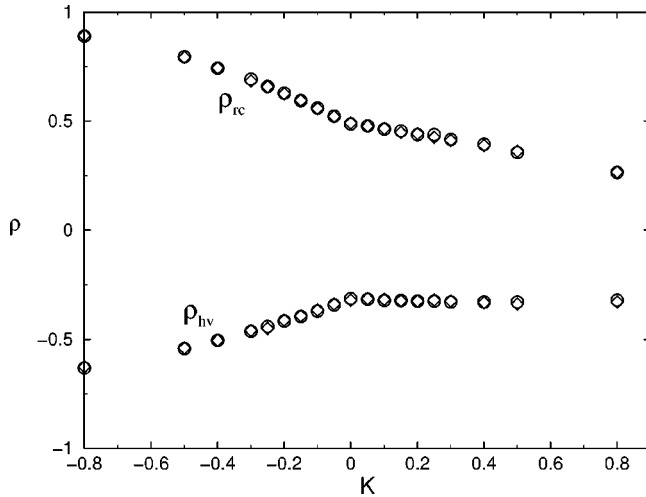


FIG. 17. The difference in the expectation value of sharp hill tops and of sharp valley bottoms, ρ_{hv} , and local sharp ridges and canyons, ρ_{rc} , as function of K in the 2D BCSOS model. The diamonds (circles) are for lattice size $L=36$ (64).

$=W_3/W_2^{1.5}$ and $R_4=W_4/W_2^2$ do not vary significantly with K either.

We performed quantitative MC runs at $K=\pm 0.25, \pm 0.1$ for system sizes up to $L=60$ (with 2×10^6 MC step runs after 4×10^3 initial MC steps). Figures 11, 12, and 13 show the $\alpha_n(L)$ approximants as function of $1/L$ at $K=\pm 0.25$. The $K=0$ data are included as reference. The corrections to scaling in the even moments increase with K , and are an order of magnitude smaller at $K=-0.25$. The three curves are consistent with convergence towards the same values for α_2 and α_4 . Naively these values point to an α smaller than $\frac{2}{5}$, but still consistent with the KKL value if the crossover scaling exponent is large (see Sec. III). The corrections to scaling in α_3 are less clear-cut. At first glance the three curves seem more or less parallel (which would suggest a continuous variation in α_3 with K), but they actually converge to indistinguishable values for α_3 given the error bar from the numerical MC noise.

The amplitude ratios $R_3=W_3/W_2^{3/2}$ and $R_4=W_4/W_2^2$ are shown in Figs. 14 and 15. As before, these amplitude ratios are more stable than the numerical values of α_n . The data confirm universal K -independent values of R_n (although R_4 drifts off by a few percent at $K=0.25$).

In 1D the skewness amplitude is tunable and directly related to the amount of particle-hole symmetry breaking at the microscopic level. Figures 16 and 17 show how the microscopic particle-hole asymmetry varies as function of K in the 2D BCSOS model. We measure several local quantities. Figure 16 shows the density difference ratio $\rho=(\rho_h-\rho_v)/(\rho_h+\rho_v)$ between local sharp hill tops ρ_h and local sharp valleys ρ_v as seen along 1D cross sections of the crystal. Figure 17 shows the density difference ρ_{hv} between local sharp hill tops and local sharp valleys bottoms in the 2D surface and also the difference between sharp ridges versus sharp canyons ρ_{rc} as defined in Fig. 18. All three quantities vary dramatically with K . This demonstrates that the local skewness coupling constant u_{sk} varies significantly with K , sufficiently to expect a large variation in R_3 if (macroscopic)

hill			valley			ridge			canyon		
h	h+1	h	h+2	h+1	h+2	h+2	h+1	h	h	h+1	h+2
h+1	h+2	h+1	h+1	h	h+1	h+1	h+2	h+1	h+1	h	h+1
h	h+1	h	h+2	h+1	h+2	h	h+1	h+2	h+2	h+1	h
(1)			(2)			(3)			(4)		

FIG. 18. Definition of local sharp hill tops, valley bottoms, ridges, and canyons in the 2D BCSOS model.

skewness is tunable. Since this not the case, $R_3 \approx -0.27$ is most likely a universal property of the stationary state.

The curves in Fig. 16 and Fig. 17 have kinks at $K=0$. These are caused by the definition of the deposition probabilities, $p=\min(1, \exp(-\Delta E))$. The probabilities are temperature dependent for some configurations but constant, $p=1$, for others. At $K=0$ they are being reshuffled. The curves of Fig. 10 have similar dips at $K=0$ for small L , but these vanish with system size. This is another illustration of the insensitivity of the macroscopic length scale properties of the stationary state on the local properties.

VI. CONCLUSIONS

The most important result of this paper is that the amplitude ratios $R_3=W_3/W_2^{1.5}$ and $R_4=W_4/W_2^2$ of the stationary-state moments converge to the same value in the KK and BCSOS model, $R_3=-0.27(1)$ and $R_4=+3.15(2)$. At the start of this project we expected that the skewness R_3 would be the most sensitive parameter to test the universality of the KPZ stationary-state properties in 2D. However, R_3 is numerically much more stable than the surface roughness critical exponent α . Here R_3 takes the same value in the KK and BCSOS models, and does not vary significantly in the BCSOS model with the temperature parameter K , in contrast to the strong variation in the microscopic measures of particle-hole asymmetry. The 2D KPZ stationary-state skewness is universal, unlike 1D where it is tunable.

The differences in the numerical values for α in the KK and BCSOS models have been a puzzle for a long time. The corrections to FSS scaling in the KK model are small, compared to the MC noise, and point clearly to the KKL value $\alpha=\frac{2}{5}$. The FSS corrections to scaling in the BCSOS model are large. The stationary-state roughness exponent converges naively but systematically to a smaller value $\alpha \approx 0.38$. However, our FSS analysis shows that the data are consistent with $\alpha=\frac{2}{5}$ if the leading corrections to scaling exponents are dominated by $y_{ir} \approx -0.6(2)$ for the even moments and $y_{ir} \approx -1.7(3)$ for the odd ones. These values are different, but in the same range as predicted by simple-minded power counting. This is an important issue, because different values of α in the KK and BCSOS models, and variations with K in the latter, would imply nonuniversality of 2D KPZ scaling and open up the possibility of, e.g., a continuously varying α . Our data suggest one single KPZ fixed point with unique exponents. It is most likely Lässig's stationary state.

ACKNOWLEDGMENT

This work was supported by NSF Grant No. DMR-9700430.

- [1] M. Kardar, G. Parisi, and Y-C. Zhang, Phys. Rev. Lett. **56**, 889 (1986).
- [2] J. Krug and H. Spohn, in *Solids Far from Equilibrium: Growth, Morphology and Defects*, edited by C. Godrèche (Cambridge University Press, Cambridge, England, 1991).
- [3] P. Meakin, Phys. Rep. **235**, 189 (1993).
- [4] J. Krug, in *Scale Invariance, Interfaces, and Non-Equilibrium Dynamics*, edited by A. McKane, M. Droz, J. Vannimenus, and D. Wolf (Plenum, New York, 1995).
- [5] T.J. Halpin-Healy and Y.C. Zhang, Phys. Rep. **254**, 215 (1995).
- [6] M. Lässig and H. Kinzelbach, Phys. Rev. Lett. **78**, 903 (1997); K. Wiese, Phys. Rev. E **56**, 5013 (1997); C. Castellano, M. Marsili, and L. Pietronero, Phys. Rev. Lett. **80**, 4830 (1998).
- [7] D. Dhar, Phase Transit. **9**, 51 (1987).
- [8] L-H. Gwa and H. Spohn, Phys. Rev. Lett. **68**, 725 (1992); Phys. Rev. A **46**, 844 (1992).
- [9] J. Neergaard and M. den Nijs, Phys. Rev. Lett. **74**, 730 (1995).
- [10] See, e.g., B. Derrida, M.R. Evans, V. Hakim, and V. Pasquier, J. Phys. A **26**, 1493 (1993).
- [11] J. M. Kim and J. M. Kosterlitz, Phys. Rev. Lett. **62**, 2289 (1989).
- [12] J.G. Amar and F. Family, Phys. Rev. Lett. **64**, 543 (1990); **64**, 2334 (1990); J. Krug and H. Spohn, *ibid.* **64**, 2332 (1990); J. Kim, T. Ala-Nissila, and J.M. Kosterlitz, *ibid.* **64**, 2333 (1990).
- [13] For numerical results on the 2D BCSOS model see, e.g., D. Liu and M. Plischke, Phys. Rev. B **38**, 4781 (1988); M. Koita and A.C. Levi, J. Phys. A **25**, 3121 (1992); B.M. Forrest and Lei-Han Tang, Phys. Rev. Lett. **64**, 1405 (1990); also the above review papers [2–5].
- [14] M. Lässig, Phys. Rev. Lett. **80**, 2366 (1998).
- [15] M. den Nijs and J. Neergaard, J. Phys. A **30**, 1935 (1997).
- [16] J. Krug, P. Meakin, and T. Halpin-Healy, Phys. Rev. A **45**, 638 (1992).
- [17] M. den Nijs, J. Phys. A **18**, L549 (1985).
- [18] M. den Nijs, in *The Chemical Physics of Solid Surfaces and Heterogeneous Catalysis*, edited by D. King (Elsevier, Amsterdam, 1994), Vol. 7, Chap. 4.
- [19] See, e.g., H. van Beijeren and I. Nolden, in *Structures and Dynamics of Surfaces*, edited by W. Schommers and P. von Blanckenhagen (Springer, Berlin, 1987), Vol. 2.